



OPEN

A novel monoclonal antibody against 6-sulfo sialyl Lewis x glycans attenuates murine allergic rhinitis by suppressing Th2 immune responses

Wei Liu, Wei Xiong, Wenxin Liu, Jotaro Hirakawa & Hiroto Kawashima

Lymphocyte homing is mediated by the interaction between L-selectin on lymphocytes and its glycoprotein ligands modified with 6-sulfo sialyl Lewis x (6-sulfo sLe^x) glycans on high endothelial venules (HEVs) in peripheral lymph nodes (PLNs). However, the lack of specific antibodies reactive with both human and mouse 6-sulfo sLe^x has limited our understanding of its function in vivo. Here, we generated a novel monoclonal antibody, termed SF1, that specifically reacts with 6-sulfo sLe^x expressed on HEVs in both species in a manner dependent on sulfate, fucose, and sialic acid modifications. Glycan array and biolayer interferometry analyses indicated that SF1 specifically bound to 6-sulfo sLe^x with a dissociation constant of 6.09×10^{-9} M. SF1 specifically bound to four glycoproteins from PLNs corresponding to the molecular sizes of L-selectin ligand glycoproteins. Consistently, SF1 inhibited L-selectin-dependent lymphocyte rolling on 6-sulfo sLe^x-expressing cells ex vivo and lymphocyte homing to PLNs and nasal-associated lymphoid tissues in vivo. Furthermore, SF1 significantly attenuated ovalbumin-induced allergic rhinitis in mice in association with significant suppression of Th2 immune responses. Collectively, these results suggest that SF1 can be useful for the functional analysis of 6-sulfo sLe^x and may potentially serve as a novel therapeutic agent against immune-related diseases.

Lymphocytes continuously circulate in the body via the blood and lymph to monitor for foreign antigens¹⁻³. Lymphocyte homing is a phenomenon in which circulating lymphocytes in peripheral blood migrate to secondary lymphoid organs, such as peripheral lymph nodes (PLNs), where immune responses occur. Lymphocyte homing to PLNs is critically dependent on the interaction between the homing receptor, L-selectin, expressed on the surface of lymphocytes and 6-sulfo sialyl Lewis x (6-sulfo sLe^x; sialic acid α 2-3Gal β 1-4[Fuca1-3(sulfo-6)]GlcNAc β 1-R; Fig. 1a) expressed on the surface of specialized endothelial venules, called high endothelial venules (HEVs), as revealed by studies using sialidase^{4,5} and in α 2,3-sialyltransferase-deficient⁶, α 1,3-fucosyltransferase (FucT)-IV and -VII double-deficient (FucT-IV/-VII DKO)⁷, and *N*-acetylglucosamine-6-*O*-sulfotransferase (GlcNAc6ST)-1 and -2 double-deficient (GlcNAc6ST-1/-2 DKO) mice^{8,9}. The structural difference between 6-sulfo sLe^x expressed in humans and mice is as follows: 6-sulfo sLe^x expressed in humans is exclusively modified with *N*-acetylneuraminic acid (Neu5Ac) because of the lack of the gene encoding CMP-Neu5Ac hydroxylase (Cmah) in humans¹⁰ which converts CMP-Neu5Ac to CMP-Neu5Gc, whereas that expressed in mice is modified with *N*-glycolylneuraminic acid (Neu5Gc) due to the expression of Cmah¹¹. To date, the lack of specific antibodies reactive with both human and mouse 6-sulfo sLe^x has limited our understanding of its expression and functions in lymphocyte homing and immune-related diseases.

MECA-79¹², a mAb widely used as a marker for human and mouse HEVs in PLNs, binds to 6-sulfo sLe^x only when it is present on a specific glycan core structure and recognizes extended core 1 *O*-glycans containing 6-sulfo *N*-acetylglucosamine (6-sulfo sialyl LacNAc, sialic acid α 2-3Gal β 1-4GlcNAc β 1-R) as its minimum epitope¹³. Previously developed mAbs, S1 and S2, also bind to 6-sulfo sLe^x, but they recognize *O*-glycans containing 6-sulfo LacNAc and *N*- and *O*-glycans containing 6-sulfo LacNAc, respectively, as their minimum epitopes¹⁴. Similarly, mAb CL40 is reactive with 6-sulfo sLe^x, which binds to both *N*- and *O*-glycans containing 6-sulfo LacNAc as its

Laboratory of Microbiology and Immunology, Graduate School of Pharmaceutical Sciences, Chiba University, 1-8-1 Inohana, Chuo-Ku, Chiba 260-8675, Japan. ✉email: h-kawashima@chiba-u.jp

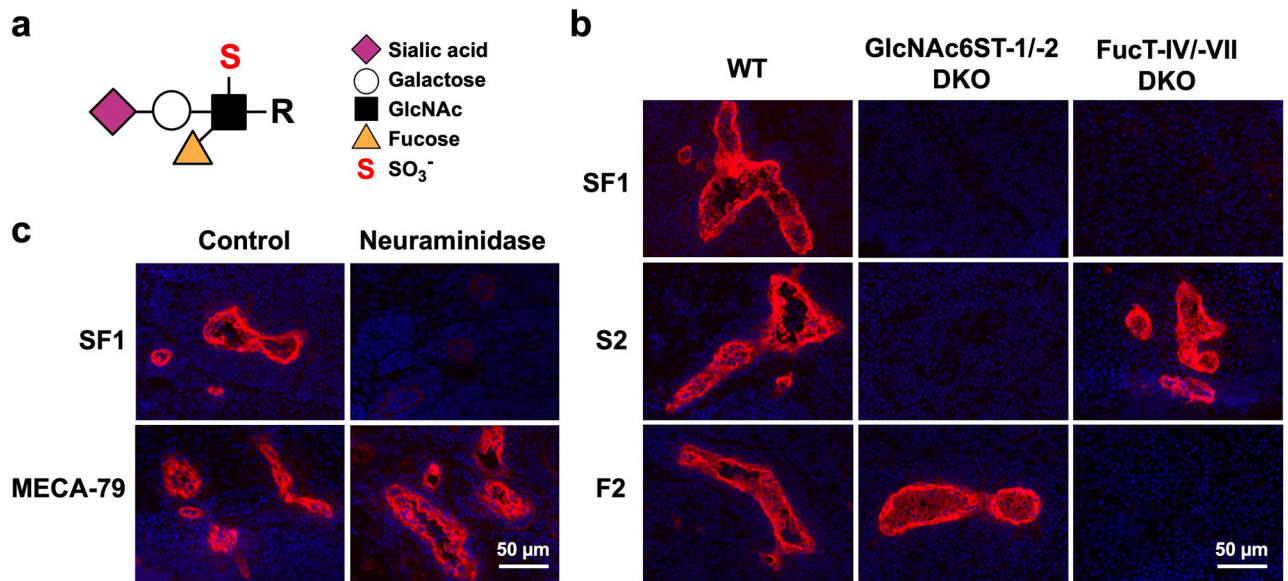


Figure 1. Immunofluorescence of PLN tissue sections from various strains of mice with anti-glycan mAbs. **(a)** Structure of 6-sulfo sLe^x. **(b)** Immunofluorescence. Frozen sections of PLNs from C57BL/6 WT, GlcNAc6ST-1/-2 DKO, and FucT-IV/-VII DKO mice were incubated with biotinylated SF1, S2, or F2, followed by incubation with streptavidin-Alexa Fluor 594 (red) and DAPI (blue). **(c)** Effects of neuraminidase on mAb binding. Frozen sections of PLNs from C57BL/6 WT mice that had been treated with (*Neuraminidase*) or without (*Control*) α 2-3,6,8 neuraminidase were stained with biotinylated SF1 or MECA-79 as in **(b)**. Bars, 50 μ m.

epitope¹⁵. MAb F1 and F2 also bind to 6-sulfo sLe^x, but recognize *N*- and *O*-glycans containing sialyl Lewis x (sLe^x; sialic acid α 2-3Gal β 1-4[Fuca1-3]GlcNAc β 1-R) as their minimum epitopes¹⁶. Although these mAbs can react with both human and mouse 6-sulfo sLe^x expressed on HEVs and with a portion of the 6-sulfo sLe^x structure as their epitopes, none of them are specific to 6-sulfo sLe^x. One mAb, G152, reacts specifically with the 6-sulfo sLe^x structure expressed in humans¹⁷; however, this mAb cannot bind to 6-sulfo sLe^x expressed in mice, and thus its effects on lymphocyte homing and immune-related diseases in mice cannot be determined. This is possibly because G152 selectively binds to glycans modified with Neu5Ac expressed in humans, whereas it fails to bind to glycans modified with Neu5Gc that is abundantly expressed in mice.

We previously established an efficient method for the generation of anti-glycan mAbs using glycosyltransferase- or sulfotransferase-deficient mice, based on the high immunogenicity of the missing glycans in mutant mice^{14,16,18}. In addition, by immunizing mutant mice with transfectants overexpressing not only the missing enzymes but also Cmah¹¹, we were able to generate mAbs reactive with both humans and mice. Based on this methodology, we herein generated a novel anti-6-sulfo sLe^x mAb, termed SF1, that reacts with both human and mouse 6-sulfo sLe^x. SF1 bound specifically to human and mouse HEVs and efficiently blocked lymphocyte homing to PLNs and nasal-associated lymphoid tissues (NALTs) in mice. We also showed that SF1 suppressed ovalbumin (OVA)-induced allergic rhinitis in mice, suggesting its potential for the functional analysis of 6-sulfo sLe^x under physiological and pathophysiological conditions. Hence, SF1 may serve as a novel therapeutic agent against immune-related diseases.

Results

Generation of mAb SF1 reactive with 6-sulfo sLe^x

To obtain an anti-6-sulfo sLe^x mAb, GlcNAc6ST-1/-2 DKO mice were immunized with Chinese hamster ovary (CHO) cells stably expressing 6-sulfo sLe^x that had been transiently transfected with an expression vector encoding Cmah. Splenocytes of immunized mice were fused with mouse P3X63Ag8.653 myeloma cells to generate hybridomas. The culture supernatants were screened for immunoreactivity with the HEVs of WT mice and for the lack of immunoreactivity with the HEVs of GlcNAc6ST-1/-2 DKO⁸ and FucT-IV/-VII DKO⁷ mice lacking 6-sulfo sLe^x. As a result, one hybridoma clone secreting anti-6-sulfo sLe^x mAb SF1 (mouse IgG₁, κ) was established.

To compare the carbohydrate-binding specificity of mAb SF1 with that of previously established mAbs reactive with mouse HEVs, immunofluorescence staining of PLN frozen sections using biotinylated mAbs was performed (Fig. 1b). SF1 strongly bound to the HEVs of WT mice, but not to those of GlcNAc6ST-1/-2 DKO or FucT-IV/-VII DKO mice, indicating that SF1 requires both GlcNAc-6-*O*-sulfate and α 1,3-fucose modifications. In contrast, the binding of mAbs S2¹⁴ and F2¹⁶ to HEVs was exclusively eliminated in GlcNAc6ST-1/-2 DKO and FucT-IV/-VII DKO mice, respectively, indicating that these mAbs require either sulfate or α 1,3-fucose, but not both modifications. The staining of HEVs by SF1 was significantly diminished after neuraminidase treatment of the frozen sections, whereas that by mAb MECA-79¹² was unaffected (Fig. 1c), indicating that SF1 also requires

the sialylation of glycans. Collectively, these results indicate that SF1 binds to HEVs in mouse PLNs in a manner dependent on the sulfate, fucose, and sialic acid modifications.

Glycan-binding specificity and dissociation constant of SF1

To determine the glycan-binding specificity of SF1 in more detail, glycan array analysis was performed. SF1 specifically bound to 6-sulfo sLe^x (Glycan #253) among all glycans on the array (Supplementary Table S1). Figure 2a shows the results of 6-sulfo sLe^x and other representative glycans with related structures on the array. In contrast to mAbs S1 and S2¹⁴, SF1 did not bind to 6-sulfo sialyl LacNAc (Glycan #252), indicating that α 1,3-fucose is required for binding. Similarly, in contrast to mAbs F1 and F2¹⁶, SF1 failed to bind to sLe^x (Glycan #255), indicating that the sulfate group is also required for binding. Consistent with the results of sialidase treatment described above, SF1 did not bind to 6-sulfo Lewis x (Glycan #291), lacking terminal α 2,3-linked sialic acid. Substitution of sialic acid with sulfate at 3-OH of the galactose residue (Glycan #220) resulted in the complete loss of binding. In addition, SF1 did not bind to 6'-sulfo sLe^x (Glycan #231), which was previously reported to interact with L-selectin¹⁹, or α 1-2 fucosylated 6-sulfo LacNAc (Glycan #222), which is present in the O-glycans of murine colonic mucins²⁰. Consistently, SF1 did not bind to LacNAc (Glycan #170), sialyl LacNAc (Glycan #261), and disulfated LacNAc (Glycan #445). Collectively, these results indicate that SF1 is highly specific to 6-sulfo sLe^x glycan.

To determine the dissociation constant (K_d) of the binding between SF1 and 6-sulfo sLe^x, we performed biolayer interferometry using Octet RED96 (Fig. 2b). Using streptavidin-coupled biosensor tips that had been pre-incubated with biotinylated 6-sulfo sLe^x, the association rate constant (K_{on}) and dissociation rate constant (K_{off}) were determined to be 9.56×10^5 (1/Ms) and 5.82×10^{-3} (1/s), respectively. We did not detect any binding of SF1 to biotinylated sialyl LacNAc, confirming that the specificity of the binding of SF1 to 6-sulfo sLe^x. K_d was calculated as K_{off}/K_{on} . The K_d value of the binding between SF1 and 6-sulfo sLe^x was calculated to be 6.09×10^{-9} (M).

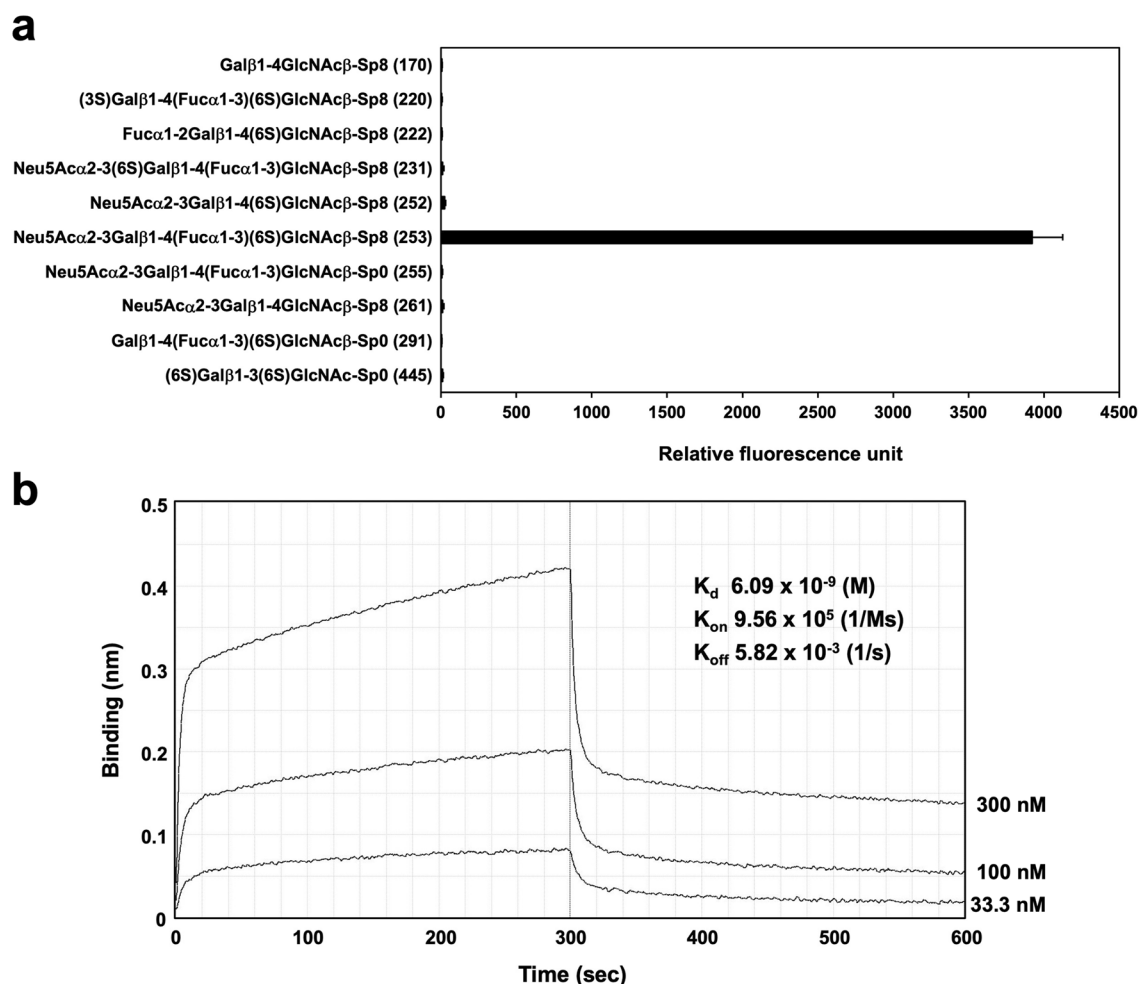


Figure 2. Glycan array analysis and biolayer interferometry of the binding between SF1 and 6-sulfo sLe^x. (a) Glycan array of the Consortium for Functional Glycomics was probed with SF1. Error bars represent the mean \pm standard deviation (SD) of four measurements. Glycan numbers are shown in parentheses after their structures. (b) Biolayer interferometry using Octet RED96. Binding of SF1 (33.3, 100, and 300 nM) was measured using streptavidin-coupled biosensor tips coated with biotinylated 6-sulfo sLe^x.

Inhibitory effects of SF1 on L-selectin-Fc binding to HEVs and lymphocyte rolling

Since 6-sulfo sLe^x functions as a major ligand for L-selectin, we examined the blocking effects of SF1 on the binding of L-selectin to its ligands on HEVs. To this end, frozen sections of mouse PLNs were incubated with the L-selectin-Fc fusion protein in the presence or absence of SF1, followed by incubation with biotinylated anti-human IgG secondary antibody and Alexa Fluor 594-labeled streptavidin (Fig. 3a). SF1 strongly inhibited the binding of L-selectin-Fc to HEVs, indicating that SF1 inhibits the interaction between the lymphocyte homing receptor, L-selectin, and its ligands expressed on HEVs.

To determine whether SF1 blocks L-selectin-mediated lymphocyte rolling under physiological flow conditions, a parallel-plate flow chamber assay was performed. As shown in Fig. 3b, CHO cells expressing CD34 core proteins and 6-sulfo sLe^x glycans supported the L-selectin-dependent rolling of mouse lymphocytes, which was completely blocked by the anti-L-selectin mAb MEL-14²¹ under physiological shear stress. As a result, the rolling was significantly inhibited by SF1, indicating that SF1 has the ability to block the interaction between L-selectin and its ligands under physiological shear stress.

Binding of SF1 to L-selectin ligand glycoproteins and its blocking effects on lymphocyte homing to PLNs

L-selectin interacts with a unique set of glycoproteins, termed peripheral node addressins²², such as Sgp200²³, podocalyxin-like protein²⁴, CD34²⁵, and glycosylation-dependent cell adhesion molecule-1 (GlyCAM-1)²⁶. To determine whether SF1 binds to these glycoproteins, we performed western blotting analysis using tissue lysates of PLNs from WT, GlcNAc6ST-1/-2 DKO, and FucT-IV/-VII DKO mice (Fig. 4a, Supplementary Fig. S1). Consistent with the ability of SF1 to block the binding of L-selectin to its ligands on HEVs, SF1 mainly bound to four glycoproteins corresponding to the molecular sizes of the peripheral node addressins in WT mice, but not those from GlcNAc6ST-1/-2 or FucT-IV/-VII DKO mice lacking 6-sulfo sLe^x.

To assess the functional effects of SF1 in vivo, a lymphocyte homing assay using C57BL/6 WT mice was performed. As shown in Fig. 4b, SF1 inhibited lymphocyte homing to PLNs (containing cervical lymph nodes [CLNs], brachial lymph nodes [BLNs], and inguinal lymph nodes [ILNs]) by more than 90%. Homing to the mesenteric lymph nodes (MLNs) was also suppressed by approximately 60%. In contrast, SF1 did not show any inhibitory effects on lymphocyte homing to Peyer's patches (PPs) and spleen. Consistent with these findings, SF1 clearly bound to HEVs in PLNs and MLNs, but minimally bound to those in PP (Fig. 4c).

Suppressive effects of SF1 on lymphocyte homing to NALTs and a murine allergic rhinitis model

NALT is a secondary lymphoid organ in mice, where immune responses against inhaled allergens primarily occur²⁷. To determine the effects of SF1 in a murine allergic rhinitis model, we examined the reactivity of SF1 to HEVs in NALTs using immunofluorescence. As shown in Fig. 5a, HEVs in NALTs of C57BL/6 mice were reactive with SF1, which was eliminated in GlcNAc6ST-1/-2 and FucT-IV/-VII DKO mice. In addition, HEVs in the NALTs of BALB/c mice were also strongly reactive with SF1. Because BALB/c mice are T helper 2 (Th2)-prone and are often used for murine models of allergy²⁸, we used this mouse strain for further analysis of lymphocyte homing and OVA-induced allergic rhinitis model. In the homing assay using BALB/c mice, each secondary lymphoid organ was collected separately (Fig. 5b). Similar to what was observed in C57BL/6 mice, lymphocyte homing to PLNs (CLNs, BLNs, and ILNs) was strongly blocked by SF1 by >95%, whereas that to MLNs was partially blocked by 60%, and that to PP and spleen was unaffected by SF1. Consistent with the immunofluorescence data, SF1 significantly inhibited lymphocyte homing to NALTs by >95%.

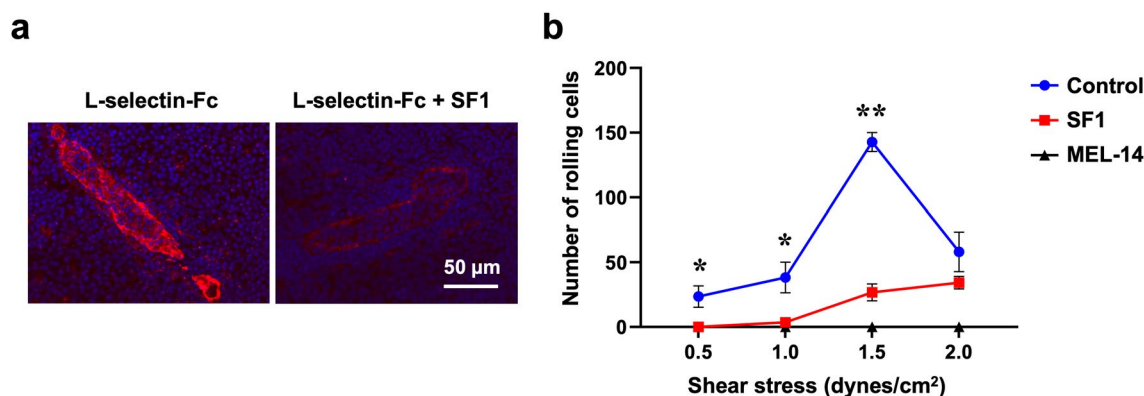


Figure 3. Effects of SF1 on the binding of L-selectin-Fc to HEVs in PLN sections and L-selectin-mediated lymphocyte rolling. (a) Binding of L-selectin-Fc to PLN HEVs in C57BL/6 WT mice in the presence (+SF1) or absence of SF1. (b) The number of rolling cells was counted for 60 s at shear stresses of 0.5, 1.0, 1.5, and 2.0 dynes/cm². Lymphocytes from mouse spleens that had been pretreated with or without MEL-14 were introduced into the flow chamber with the bottom surface covered with a monolayer of CHO/CD34/C1/C2/FucT-7/GlcNAc6ST-2 cells that had been pretreated with or without SF1. Error bars represent the standard error of the four measurements. * $P < 0.05$, ** $P < 0.01$ (SF1 vs. Control).

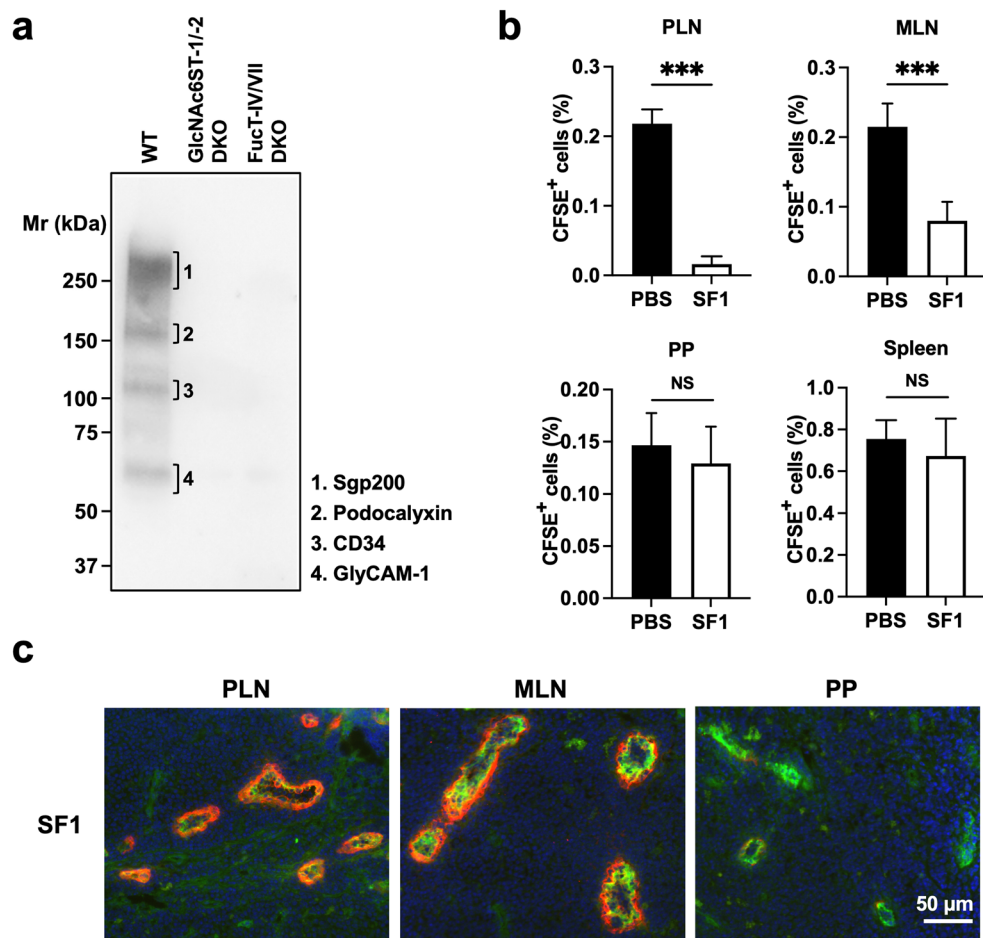


Figure 4. SF1 specifically binds to four glycoproteins and inhibits lymphocyte homing to PLNs and MLNs in C57BL/6 mice. **(a)** Western blotting. The blots of PLN lysates from C57BL/6 WT, GlcNAc6ST-1/-2 DKO, or FucT-IV/-VII DKO mice were probed with SF1, followed by HRP-conjugated anti-mouse IgG that specifically reacts with undenatured mouse IgG. **(b)** Inhibition of lymphocyte homing by SF1 in C57BL/6 mice. CFSE-labeled lymphocytes from C57BL/6 WT mice were injected into the tail veins of the same strain of WT mice that had been pre-injected with SF1 or PBS 2 h before the injection of labeled lymphocytes. Lymphocyte homing to PLNs (containing CLNs, BLNs, and ILNs), MLNs, PPs, and spleen is shown as the percentage of CFSE⁺ lymphocytes among the total lymphocytes in each lymphoid organ (n = 5). Each bar represents the mean ± SD. ****P* < 0.001; NS not significant. **(c)** Immunofluorescence: Frozen sections of PLNs, MLNs, and PPs from C57BL/6 WT mice were incubated with biotinylated SF1 and Alexa Fluor 488-conjugated anti-mouse CD31 (green), streptavidin-Alexa Fluor 594 (red), and DAPI (blue). Bar, 50 μm.

To determine the effects of SF1 on allergic rhinitis in mice, we induced allergic rhinitis in BALB/c mice via the intranasal administration of OVA in the presence or absence of SF1 (Fig. 6a) and examined their clinical symptoms. The number of sneezes and nose scratches after the final intranasal immunization with OVA was significantly diminished in SF1-administered mice (Fig. 6b). Consistently, the levels of OVA-specific serum IgE, a key immunoglobulin that causes allergic symptoms, were diminished in SF1-administered mice (Fig. 6c). The levels of OVA-specific IgG1 produced by Th2 immune responses, similar to IgE, were also reduced, whereas those of OVA-specific IgG2a produced by Th1 immune responses were increased, suggesting that Th2 immune responses are specifically blocked in OVA-induced allergic rhinitis.

To determine the molecular basis of this suppression, we performed reverse transcription-quantitative PCR (RT-qPCR) analysis using total RNAs from NALTs and CLNs, where intranasally administered antigens were accumulated (Fig. 7a,b). The expression levels of Th2 cytokine, interleukin (IL)-4, which is critical for IgE class switching²⁹, were significantly reduced by SF1 administration in both NALTs and CLNs. The levels of another Th2 cytokine, IL-5, were also significantly reduced by SF1 in NALTs, although the reduction in CLN levels was not statistically significant. In contrast, the expression levels of the immunosuppressive cytokine IL-10, which is secreted from regulatory T (Treg) cells³⁰ were increased by SF1 administration in both NALTs and CLNs. Consistently, the expression levels of forkhead box P3 (Foxp3), a master transcription factor critical for the development and maintenance of Treg cells³¹, was increased by SF1 administration.

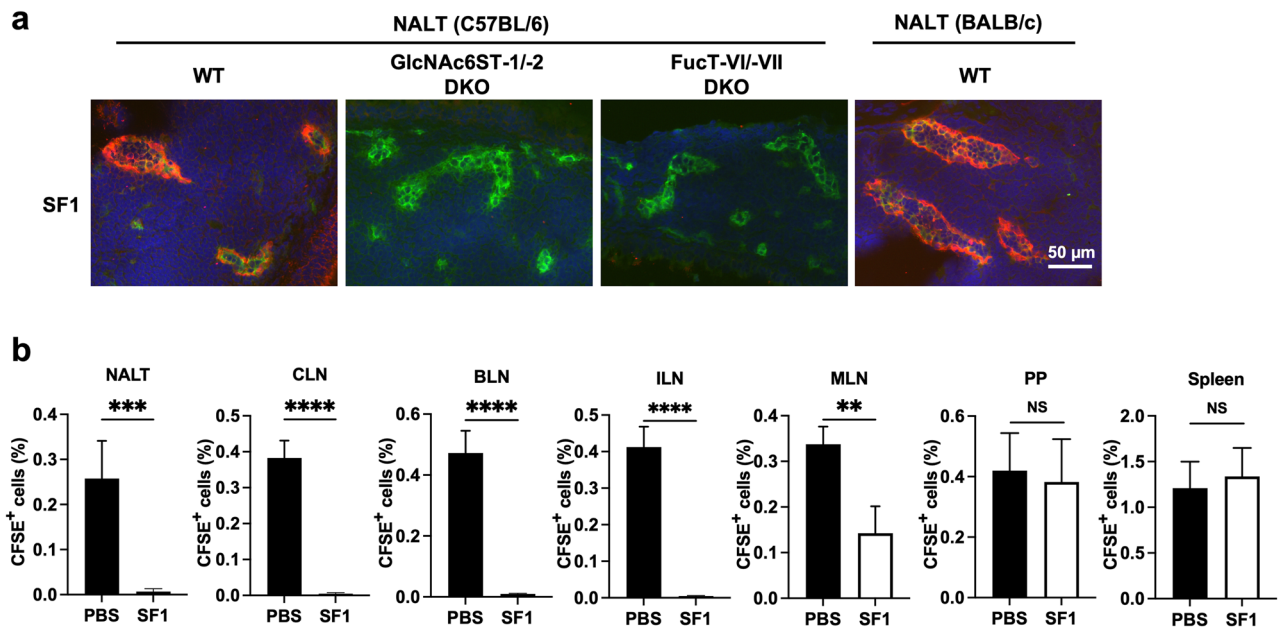


Figure 5. Binding of SF1 to NALT HEVs and its effect on lymphocyte homing in BALB/c mice. (a) Immunofluorescence: Frozen sections of NALTs from C57BL/6 WT, GlcNAc6ST-1/-2 DKO, FucT-IV/-VII DKO, and BALB/c WT mice were incubated with biotinylated SF1 and Alexa Fluor 488-conjugated anti-mouse CD31 (green), streptavidin-Alexa Fluor 594 (red), and DAPI (blue). Bar, 50 μ m. (b) Inhibition of lymphocyte homing by SF1 in BALB/c mice. CFSE-labeled lymphocytes from BALB/c WT mice were injected into the tail veins of the same strain of WT mice that had been pre-injected with SF1 or PBS 2 h before the injection of labeled lymphocytes. Lymphocyte homing is shown as the percentage of CFSE⁺ lymphocytes among the total lymphocytes in each lymphoid organ. Each bar represents the mean \pm SD (n = 4). ** P < 0.01; *** P < 0.001; **** P < 0.0001; NS not significant.

Immunohistochemical staining of normal human tissues with SF1

To confirm the tissue-binding specificity of SF1, immunohistochemical staining of normal human tissues with SF1 was performed. As shown in Fig. 8, SF1 showed no staining in the aorta, mammary gland, cerebellum, cerebrum, heart, lung, small intestine, large intestine, skin, and spleen, but selectively stained the lymph nodes and tonsils. From the enlarged photographs, it was confirmed that SF1 specifically binds to HEVs in these lymphoid organs. Because human lymphocytes are selectively recruited to these lymphoid organs via HEVs to evoke immune responses, these results, together with the abovementioned effects of SF1 on lymphocyte homing and the murine allergic rhinitis model, suggest that SF1 may be useful as a therapeutic agent against immune-related diseases in humans.

Discussion

In the present study, we established a novel mAb against 6-sulfo sLe^x, termed SF1, using a previously established method to generate anti-glycan mAbs by immunizing mice deficient in glycan-synthesizing enzymes with transfectants that overexpress the missing enzymes^{14,18}. Here, we provide biochemical evidence of the specificity and affinity by glycan array and bilayer interferometry analyses. We also provide evidence that SF1 selectively binds to L-selectin ligand glycoproteins and inhibits L-selectin-mediated rolling. In vivo functional analyses indicated that SF1 significantly inhibited lymphocyte homing to PLNs and NALTs, and allergic rhinitis in mice. Together with the results of histochemical analysis of human tissue sections using SF1, the results of this study suggest that 6-sulfo sLe^x can serve as a therapeutic target against immune-related diseases.

Thus far, mAb MECA-79¹² has frequently been used as a marker for HEVs. However, MECA-79 recognizes the sulfated extended core 1 structure, and its epitope does not completely match with that recognized by L-selectin containing sulfate, fucose, and sialic acid. Previously established mAbs, including S1, S2, F1, F2, and CL41, all recognize a portion of the 6-sulfo sLe^x structure^{14–16}, although they can bind both to human and mouse HEVs. Another mAb, G152, binds to the 6-sulfo sLe^x structure¹⁷; however, because of its lack of reactivity to HEVs in mice, it cannot be used to assess the in vivo function of this glycan epitope in mouse models. In contrast to these previously established mAbs, SF1 is highly specific to the 6-sulfo sLe^x structure expressed in both humans and mice, as assessed using immunofluorescence and glycan array analyses.

In our western blotting analysis, SF1 preferentially bound to glycoprotein species of > 200, 170, 100, and 60 kDa, which were probably Sgp200²³, podocalyxin-like protein²⁴, CD34²⁵, and GlyCAM-1²⁶, respectively. Although previous studies have revealed that these glycoproteins are modified with MECA-79-reactive glycans^{22,23}, it is unclear whether they can be modified with 6-sulfo sLe^x, except for GlyCAM-1, whose detailed glycan structural analysis has been performed⁸. The use of SF1 in this study suggests that these glycoproteins are indeed modified

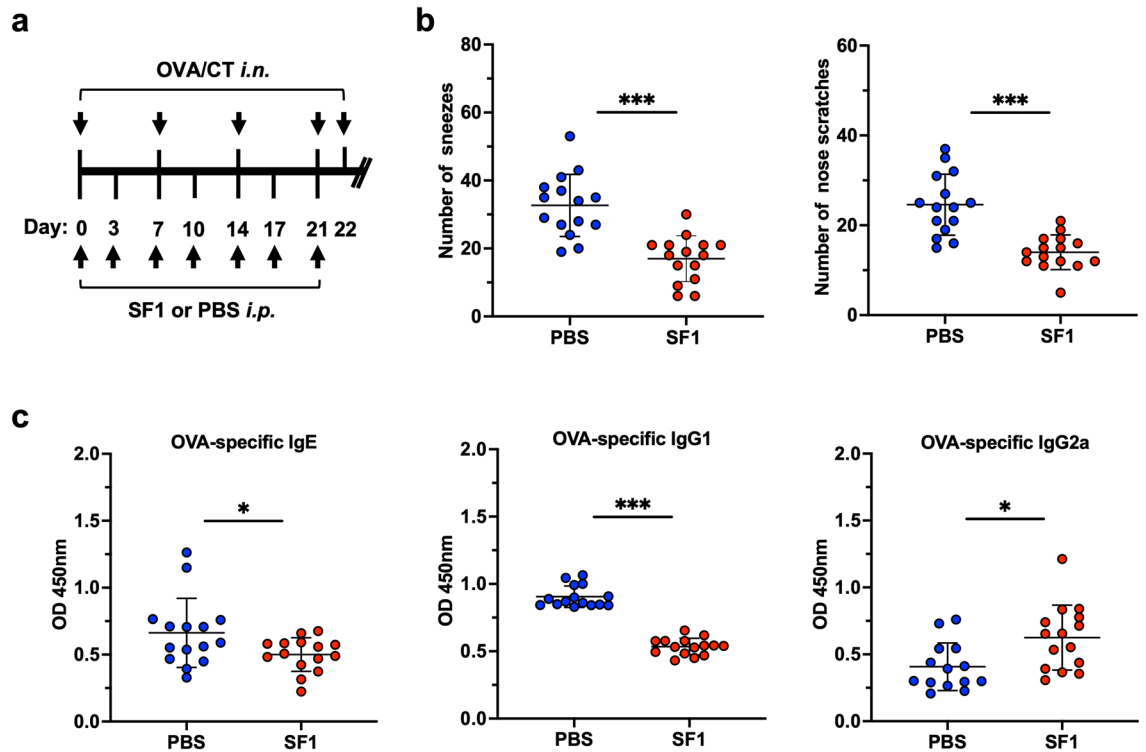


Figure 6. Effects of SF1 on OVA-induced allergic rhinitis in BALB/c mice. (a) Scheme of the OVA-induced allergic rhinitis model and SF1 administration in BALB/c mice. BALB/c WT mice were immunized intranasally (*i.n.*) with OVA and CT on days 0, 7, 14, and 21. SF1 or PBS was administered intraperitoneally (*i.p.*) on days 0, 3, 7, 10, 14, 17, and 21. On day 22, the mice received the final intranasal administration of a mixture of OVA and CT. (b) Clinical symptoms of allergic rhinitis. Immediately after the final intranasal administration of OVA and CT on day 22, the frequency of sneezing and nasal rubbing motion was measured for 12 min. (c) OVA-specific IgE, IgG1, and IgG2a levels. Sera were collected on day 22 after the final antigen administration, and ELISA was performed to detect OVA-specific antibodies. Each bar represents the mean \pm SD ($n = 14-15$). * $P < 0.05$; *** $P < 0.001$.

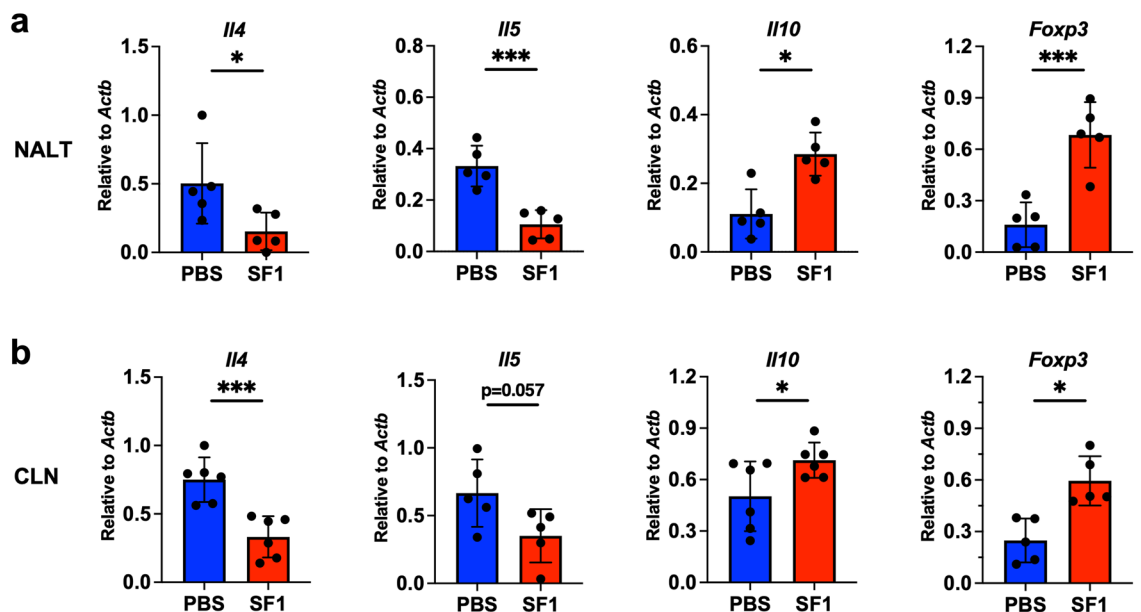


Figure 7. Effects of SF1 on the expression levels of cytokines and Foxp3 in allergic rhinitis-induced BALB/c mice. RT-qPCR analysis of the genes encoding IL-4 (*Il4*), IL-5 (*Il5*), IL-10 (*Il10*), and Foxp3 (*Foxp3*) was performed using total RNA samples from NALTs (a) and CLNs (b) collected 22 days after the final administration of OVA and CT, as shown in Fig. 6a. The expression of each gene was normalized to that of β -actin (*Actb*) using the $\Delta\Delta C_t$ method. Each bar represents the mean \pm SD ($n = 5-6$). * $P < 0.05$; *** $P < 0.001$.

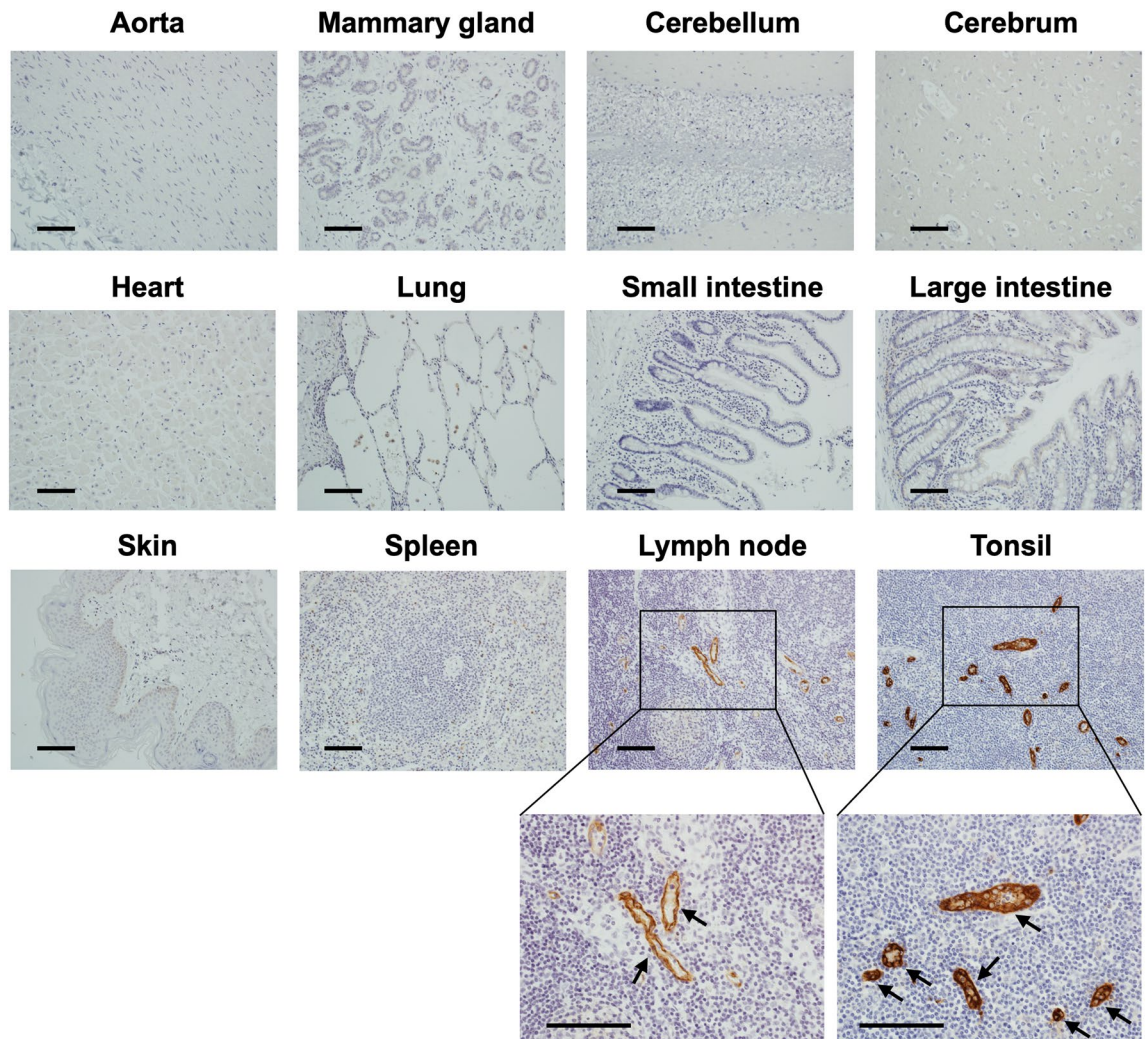


Figure 8. Immunohistochemical staining of paraffin-embedded normal human tissues with SF1. The SF1 antibody showed no binding in the aorta, breast, cerebellum, cerebrum, heart, lung, small intestine, large intestine, skin, or spleen, whereas it selectively bound to HEVs in the lymph nodes and tonsils of normal human tissues. *Arrows* in the enlarged images of the lymph nodes and tonsils indicate the HEVs. *Bars*, 100 μm .

with 6-sulfo sLe^x, although their precise core protein and glycan structures remain elusive because of the small quantities available from the murine lymph nodes.

Notably, SF1 is an IgG1 class antibody with a K_d of 6.09×10^{-9} M toward 6-sulfo sLe^x glycan. Because L-selectin is known to bind to one of its glycoprotein ligands, GlyCAM-1, with a K_d of 1.08×10^{-4} M³², the affinity of SF1 toward 6-sulfo sLe^x glycan may be high enough to block L-selectin and its ligand interaction. Consistently, our immunofluorescence study using L-selectin-Fc and ex vivo rolling assays showed that SF1 inhibited L-selectin and its ligand interaction. Furthermore, SF1 strongly inhibited lymphocyte homing to PLNs by more than 90% in both C57BL/6 and BALB/c mice, which is known to be mediated by the interaction between L-selectin and its ligands³³. In contrast, previous studies using GlcNAc6ST-1/-2 DKO mice indicated that lymphocyte homing to PLNs in these mutant mice was diminished by 75% and the remaining homing activity appeared to be mediated by unsulfated sLe^x^{8,9}. One possible explanation for the greater suppressive activity of SF1 on lymphocyte homing than that observed in DKO mice is that SF1 may also block the weak interaction between L-selectin and unsulfated sLe^x by steric hindrance. Another possibility is that unsulfated sLe^x may support significant levels of lymphocyte homing only when it is overexpressed in the absence of GlcNAc6ST-1 and -2, as evidenced by the glycan structural study of GlyCAM-1 in DKO mice⁸. These possibilities are not mutually exclusive and both may be involved. In either case, the strong blocking ability of SF1 on lymphocyte homing to PLNs warrants its possible use as an immunomodulatory agent against immune-related diseases.

SF1 did not show any inhibition of lymphocyte homing to PPs, most likely because it is mainly mediated by the interaction between $\alpha 4\beta 7$ integrin and mucosal addressin cell adhesion molecule-1 (MAdCAM-1)³⁴ and also because SF1 bound only very weakly (less than 5%) to HEVs in PPs. The partial inhibition of SF1 on lymphocyte homing to MLNs is probably because it is mediated by both L-selectin and its ligand interaction and $\alpha 4\beta 7$ integrin and MAdCAM-1 interaction³⁵. NALT is a mucosal lymphoid tissue in rodents that is equivalent to Waldeyer's

ring in humans, including the tonsils and adenoids²⁷. Consistent with our previous study using GlcNAc6ST-1/-2 DKO mice³⁶, SF1 significantly blocked lymphocyte homing to NALT by more than 95%, although PPs and NALT are the two main constituents of mucosa-associated lymphoid tissue (MALT) and are important inductive sites for mucosal immunity against ingested and inhaled antigens, respectively³⁷. Since SF1 is strongly reactive with human tonsils, it may suppress both mouse and human nasal allergic responses without affecting the immune responses against ingested antigens in PPs.

In a murine allergic rhinitis model, SF1 suppressed symptoms, such as sneezing and nose scratching, after nasal administration of the antigen in association with the reduction of antigen-specific IgE that causes allergic symptoms. SF1 also suppressed the expression of the Th2 cytokine, IL-4, which is critical for IgE class switching in B cells³⁸. These results suggest that the blockage of lymphocyte homing to NALTs and CLNs by SF1 reduced the chance of lymphocytes encountering their cognate antigens, leading to diminished Th2-cell differentiation in these lymphoid organs. Another observation is that the expression levels of the immunosuppressive cytokine, IL-10, and Treg-specific transcription factor, Foxp3³¹, were increased in NALTs and CLNs in SF1-administered mice, consistent with our previous study using GlcNAc6ST-1/-2 DKO mice³⁶. We previously reported that the homing of Treg cells to NALT is less dependent on L-selectin and its ligand interaction and more dependent on P-selectin glycoprotein ligand 1–P-selectin and CD44–hyaluronic acid interactions compared to that of conventional T cells^{1,36}. Therefore, we speculated that homing of Treg cells may have been less affected by SF1, which may be involved, at least partly, in the suppression of Th2 responses by SF1 in these lymphoid organs.

Because SF1 binds not only to mouse, but also to human tissues, it can be useful for the histopathological staining of human clinical samples. In particular, it will be interesting to examine the staining of SF1 using specimens of immune-related diseases in which HEV-like blood vessels are ectopically induced at the sites of chronic inflammation^{3,39–42} including rheumatoid arthritis⁴³, Sjögren syndrome⁴⁴, and ulcerative colitis⁴⁵. Because SF1 strongly blocks L-selectin-mediated lymphocyte homing and recruitment, determination of the expression of 6-sulfo sLe^x in HEV-like blood vessels at sites of chronic inflammation in clinical samples may lead to a novel therapeutic intervention against these diseases in the future.

In conclusion, we developed a novel anti-6-sulfo sLe^x mAb SF1 that reacts with both human and mouse tissues. Since SF1 significantly blocks lymphocyte homing and allergic rhinitis in mice, future studies using SF1 will advance our understanding of the role of 6-sulfo sLe^x in health and disease.

Methods

Animals

Animal study is approved by the Animal Research Committee of Chiba University. GlcNAc6ST-1/-2 DKO¹⁴ and FucT-IV/-VII DKO mice⁷ were maintained as previously described. C57BL/6 WT, BALB/c, and BALB/c nu/nu mice were purchased from Charles River Laboratories (Yokohama, Japan). Mice were treated in accordance with the guidelines of the Animal Research Committee of Chiba University. The reporting in the manuscript follows the recommendations in the ARRIVE (Animals in Research: Report-ing In Vivo Experiments) guidelines⁴⁶.

Generation of mAb SF1

CHO cells stably expressing human CD34, human Core1 β 1,3-*N*-acetylglucosaminyl transferase (GlcNAcT), human Core2 β 1,6-GlcNAcT-I, human FucT-VII, and mouse GlcNAc6ST-2 (CHO/CD34/C1/C2/FucT-7/GlcNAc6ST-2 cells) were transiently transfected with mouse Cmah using the FuGENE 6 transfection reagent (Promega, Madison, WI, USA). After 48 h, the cells were suspended in PBS and mixed with Imject Alum (Thermo Fisher Scientific, Waltham, MA, USA) in 1:1 ratio. The mixture was injected intraperitoneally into GlcNAc6ST-1/-2 DKO mice three times at 2-week intervals. Four days after the final immunization, lymphocytes from the spleens of immunized mice were fused with P3X63Ag8.653 myeloma cells (American Type Culture Collection, Manassas, VA, USA) using PEG solution (MW 1450; Sigma-Aldrich, St. Louis, MO, USA). Hybridomas were selected in medium containing HAT supplement (Thermo Fisher Scientific). Supernatants reactive with the HEVs of WT mice, but not with those of GlcNAc6ST-1/-2 DKO and FucT-IV and -VII DKO mice, were selected via immunofluorescence using a mixture of Alexa Fluor 488-conjugated anti-mouse IgG (Thermo Fisher Scientific) and Alexa Fluor 594-conjugated anti-mouse IgM (Thermo Fisher Scientific) as secondary antibodies. Hybridomas that secreted mAbs with the desired specificity were cloned using limiting dilution. The isotype of the mAb SF1 thus obtained was IgG1 (k), as determined using an isotyping kit (GE Healthcare, Chicago, IL, USA). Hybridomas secreting SF1 were expanded and injected into BALB/c nude mice (5.0×10^6 cells/mouse) that had been pre-injected with 500 μ L/mouse of pristane (2,6,10,14-tetramethyl pentadecane; Sigma-Aldrich) a few weeks before the cell injection, and the ascitic fluid was collected. SF1 was then purified from ascitic fluid using a caproic acid (6-aminohexanoic acid; FUJIFILM Wako, Osaka, Japan) precipitation method. In certain cases, purified SF1 was biotinylated with EZ-Link Sulfo-NHS-LC-biotin (Thermo Fisher Scientific), according to the manufacturer's protocol.

Immunofluorescence

Acetone-fixed, frozen Sections (7- μ m) from mice that had been treated with or without 5,000 U/mL α 2-3,6,8 neuraminidase (NEW ENGLAND BioLabs, Inc., Ipswich, MA, USA) for 5 h at 37 °C were incubated with PBS containing 3% BSA (Sigma-Aldrich) to block non-specific binding sites, followed by incubation with 5 μ g/mL biotinylated SF1, 1 μ g/mL biotinylated F2, 5 μ g/mL biotinylated S2, or 5 μ g/mL biotinylated MECA-79 (BioLegend, San Diego, CA, USA) together with or without 2 μ g/mL Alexa Fluor 488-conjugated anti-mouse CD31 (MEC13.3, BioLegend). After washing, the sections were incubated with 0.5 μ g/mL Alexa Fluor 594-conjugated streptavidin (Thermo Fisher Scientific) and 0.5 μ g/mL 4',6-diamidino-2-phenylindole dihydrochloride (DAPI; Thermo Fisher Scientific), and mounted using Fluoromount (Diagnostic BioSystems, Pleasanton, CA, USA). For

immunofluorescence using recombinant human L-selectin-Fc chimera protein (R&D Systems, Inc., Minneapolis, MN, USA), the tissue sections were incubated with a mixture of 5 µg/mL human L-selectin-Fc fusion protein and 40 µg/mL SF1 in Buffer A (20 mM HEPES–NaOH, 150 mM NaCl, 1 mM MgCl₂, 1 mM CaCl₂, pH 7.4, containing 0.1% BSA). After overnight incubation at 4 °C, the sections were washed with Buffer A and incubated with 1 µg/mL biotinylated goat anti-human IgG F(ab')₂ with minimum cross-reactivity with bovine, horse, mouse, and rat serum proteins (Rockland Immunochemicals, Inc., Limerick, PA, USA) for 2 h at room temperature. After washing with Buffer A, the sections were incubated with 1 µg/mL Alexa Fluor 594-conjugated streptavidin (Thermo Fisher Scientific) and 0.5 µg/mL DAPI for 1 h at room temperature. All images were obtained using a fluorescence microscope (BZ-9000; KEYENCE, Osaka, Japan).

Glycan array analysis

The purified SF1 antibody was subjected to glycan array analysis using microarray slides at the Consortium for Functional Glycomics (Core H), as described previously^{14,16}. Briefly, SF1 was dialyzed against 20 mM Tris–HCl (pH 7.4), containing 150 mM NaCl. The dialyzed antibody was diluted in 20 mM Tris–HCl (pH 7.4) containing 1% BSA, 0.05% Tween 20, 150 mM NaCl, 2 mM CaCl₂, and 2 mM MgCl₂ and applied to a glycan array. After incubation, the array was incubated with FITC-labeled anti-mouse IgG antibody and its binding was detected using a fluorescence array scanner.

Biolayer interferometry

Biolayer interferometry was performed using Octet RED96 (ForteBio, Fremont, CA, USA), according to the manufacturer's protocol. Briefly, streptavidin-coupled biosensor tips were coated with 2 µM biotinylated 6-sulfo sLe^x (6(GlcNAc)-HSO₃SiaLe^x-sp-biotin, GlycoTech Co., Gaithersburg, MD, USA). As a control, 2 µM biotinylated sialyl LacNAc (Neu5Acα2-3Galβ1-4GlcNAcβ-sp-biotin, GlycoTech Co.) was used instead of biotinylated 6-sulfo sLe^x. After washing with PBS, purified SF1 at concentrations of 33.3, 100, and 300 nM was used to measure the K_{on} and K_{off} values of the binding between SF1 and 6-sulfo sLe^x. The K_d value was determined as K_{off}/K_{on} .

Rolling assay

CHO/CD34/C1/C2/FucT-7/GlcNAc6ST-2 cells stably expressing 6-sulfo sLe^x were cultured as monolayers in 35-mm culture dishes (Corning Inc., Corning, NY, USA). Freshly prepared mouse splenocytes were fluorescently labeled with 1 µM carboxyfluorescein diacetate succinimidyl ester (CFSE; Thermo Fisher Scientific) at 37 °C for 20 min and incubated with or without 10 µg/mL of purified MEL-14 (BioLegend) for 10 min at room temperature. At the same time, the dish-attached CHO/CD34/C1/C2/FucT-7/GlcNAc6ST-2 cells were incubated with or without 10 µg/mL purified SF1 for 10 min at room temperature. After incubation, the dishes were equipped with a parallel plate flow chamber (GlycoTech Co.), according to the manufacturer's instructions. CFSE-labeled splenocytes were resuspended in buffer A at a density of 5×10^5 cells/mL and introduced into the flow chamber at wall shear stresses of 0.5, 1.0, 1.5, and 2.0 dynes/cm² using a syringe pump (Model 11 Plus, Harvard Apparatus Co., Holliston, MA, USA). Images were captured using an OptiMOS Scientific CMOS camera (Teledyne Photometrics, Tucson, AZ, USA) equipped with an inverted microscope (Axiovert S100, Carl Zeiss Meditec AG, Oberkochen, Germany) and analyzed using the Fiji ImageJ software.

Western blotting

PLNs from C57BL/6 WT, GlcNAc6ST-1/-2 DKO, and FucT-IV/-VII DKO mice were mashed in ice-cold PBS containing 1% Triton X-100 and Halt Protease inhibitor cocktail (Thermo Fisher Scientific) and solubilized for 4 h with rotation at 4 °C. Lysates were centrifuged at 15,000 rpm for 10 min. The supernatants were collected and protein concentrations were determined using a BCA Protein Assay Kit (Thermo Fisher Scientific). The obtained lysates were stored at –80 °C until use. Equal amount of lysate was applied to each lane of the SDS-PAGE gel, and western blotting was performed using 2 µg/mL purified SF1 and 1:1000 diluted horseradish peroxidase (HRP)-conjugated anti-mouse IgG (GeneTex, Irvine, CA, USA) that specifically reacts with undenatured mouse IgG. After incubating the membrane with Clarity Western ECL Substrate (Bio-Rad), bands were detected using the FUSION FX7.EDGE Imaging system (Vilber Lourmat, Collègien, France).

Lymphocyte homing assay

The lymphocyte homing assay was performed as described previously with some modifications^{8,14,16}. Briefly, MLN lymphocytes and splenocytes from C57BL/6 or BALB/c WT mice were labeled with 1 µM CFSE. After washing, 1.5×10^7 labeled cells in 100 µL of sterile PBS were injected intravenously into recipient WT mice that had been pre-injected intravenously with 200 µL of 0.5 mg/mL purified SF1 mAb (100 µg per mouse, dissolved in sterile PBS) or sterile PBS 2 h before the injection of labeled lymphocytes. Two hours after the injection of the cells, the number of CFSE⁺ cells in the cell suspensions prepared from the recipient secondary lymphoid organs was determined using flow cytometry. The cells were analyzed via flow cytometry using a CytoFLEX flow cytometer (Beckman Coulter, Brea, CA, USA).

Intranasal immunization

BALB/c mice were anesthetized with isoflurane (Pfizer Inc., New York, NY, USA) and immunized intranasally on days 0, 7, 14, and 21 with 100 µg of OVA (Sigma-Aldrich) in PBS together with 0.5 µg of cholera toxin (CT; List Biological Laboratories Inc., Campbell, CA, USA), which is used as a mucosal adjuvant in a total volume of 13 µL per mouse. Mice were injected intraperitoneally with 200 µL of 0.5 mg/mL purified SF1 mAb (100 µg per mouse, dissolved in sterile PBS) or sterile PBS on days 0, 3, 7, 10, 14, 17, and 21. On day 22, mice received

the final intranasal administration of a mixture of OVA and CT, as described above, and the frequency of sneezing and nasal rubbing motions were counted for 12 min. Thereafter, serum was collected from each mouse and stored at -80°C until use for the measurement of OVA-specific antibodies. In addition, NALTs and CLNs were collected on day 22, immersed in RNAlater solution (Thermo Fisher Scientific), and stored at -80°C until use for RT-qPCR.

ELISA for the measurement of serum antibody levels

To detect OVA-specific IgE in mouse serum, wells of a 96-well ELISA plate (Costar Assay Plate, half area; CORNING) were coated overnight with $2.0\ \mu\text{g}/\text{mL}$ anti-mouse IgE (BioLegend) and the non-specific binding sites were blocked with 3% BSA in PBS for 2 h. Diluted serum samples (1:4 dilution) were then added to the wells and incubated for 2 h. After washing with 0.05% Tween 20 in PBS, $5.0\ \mu\text{g}/\text{mL}$ biotinylated-OVA labeled with EZ-Link Sulfo-NHS-LC-biotin (Thermo Fisher Scientific) was added and the wells were incubated for 1 h. After washing, $1.0\ \mu\text{g}/\text{mL}$ HRP-conjugated streptavidin was added and incubated for 1 h. After washing, 1-step Ultra ELISA substrate (Thermo Fisher Scientific) was added to each well. The reaction was stopped by adding 2 M H_2SO_4 , and the optical density at 450 nm was measured using a 96-well spectrophotometer (Spectra Rainbow Thermo; TECAN, Männedorf, Switzerland).

To detect OVA-specific IgG1 and IgG2a in the mouse serum, the wells of the 96-well ELISA plates were coated overnight with $5.0\ \mu\text{g}/\text{mL}$ OVA (Sigma-Aldrich) in PBS, and the non-specific binding sites were blocked as described above. Diluted serum samples (1:125 dilution for IgG1 and 1:25 dilution for IgG2a) were added to the wells and incubated for 2 h. After washing with 0.05% Tween 20 in PBS, $1.0\ \mu\text{g}/\text{mL}$ HRP-conjugated goat anti-mouse IgG1 (SouthernBiotech, Birmingham, AL, USA) or $1.0\ \mu\text{g}/\text{mL}$ HRP-conjugated goat anti-mouse IgG2a (SouthernBiotech) was added and the wells were incubated for 1 h. After washing, 1-step Ultra ELISA substrate was added to each well, and the reaction was stopped with 2 M H_2SO_4 . Optical density was measured at 450 nm, as described previously.

RT-qPCR

Total RNA was extracted on day 22 from the NALTs and CLNs of allergic rhinitis-induced mice, as described above, using TRIzol reagent (Thermo Fisher Scientific). cDNA was synthesized using ReverTra Ace qPCR RT Master Mix (Toyobo, Osaka, Japan) and subjected to RT-qPCR using THUNDERBIRD SYBR qPCR Mix (Toyobo). The expression of each mRNA was normalized to that of β -actin using the $\Delta\Delta\text{Ct}$ method, according to the manufacturer's instructions (CFX96 Touch Real-Time PCR Detection System; Bio-Rad Laboratories Inc., Hercules, CA, USA). The primer sets used were as follows: β -actin, 5'-CATCCGTAAAGACCTCTATGCCAAC-3' and 5'-ATGGAGCCACCGATCCACA-3'; IL-4, 5'-TCTCGAATGTAC-CAGGAGCCATATC-3' and 5'-AGCACC TTGGAAGCCCTACAGA-3'; IL-5, 5'-AGCACAGTGGTGAAAGAGACCTT-3' and 5'-TCCAATGCATAGCTG GTGATTT-3'; IL-10, 5'-CGGGAAGACAATAACTGCACCC-3' and 5'-CGGTTAGCAGTATGTTGTCCAGC-3'; and Foxp3, 5'-AGAAGTGGTGCAGTCTCTGG-3' and 5'-AGAGCTCTGTCCATTGAGGC-3'.

Immunohistochemical staining of normal human tissues

The use of human tissue sections was approved by the ethics committee of the Chiba University and all research was performed in accordance with the guidelines. Informed consent was taken from the donors for this study. In brief, paraffin-embedded normal human tissue sections were deparaffinized in xylene, rehydrated in ethanol, and retrieved by boiling in 10 mM Tris-HCl buffer (pH 8.0) containing 1 mM EDTA for 20 min in a microwave oven. Endogenous peroxidase was inactivated using methanol containing 0.3% hydrogen peroxide for 30 min. After blocking non-specific binding sites with 1% BSA in PBS, the sections were incubated with $10\ \mu\text{g}/\text{mL}$ SF1 in PBS containing 0.1% BSA at 4°C overnight. After washing, the sections were incubated with HRP-conjugated goat anti-mouse IgG (Thermo Fisher Scientific) diluted 1:100 with 5% BSA in PBS for 60 min. After washing with PBS containing 0.1% BSA, the color reaction was developed in PBS containing 0.2% 3,3'-diaminobenzidine (Dojindo Laboratories, Kumamoto, Japan) and 0.02% hydrogen peroxide for 7 min. The sections were counterstained with hematoxylin. Slides were observed under a fluorescence microscope (BZ-9000; KEYENCE).

Statistical analysis

Student's *t*-test was used to determine the statistical significance between the experimental groups. Statistical significance was set at $P < 0.05$.

Data availability

All data are available in the main manuscript and the Supporting Information file.

Received: 30 November 2022; Accepted: 17 September 2023

Published online: 21 September 2023

References

1. Kawashima, H. & Fukuda, M. Sulfated glycans control lymphocyte homing. *Ann. N. Y. Acad. Sci.* **1253**, 112–121 (2012).
2. Ager, A. High endothelial venules and other blood vessels: critical regulators of lymphoid organ development and function. *Front. Immunol.* **8**, 45 (2017).
3. Blanchard, L. & Girard, J. P. High endothelial venules (HEVs) in immunity, inflammation and cancer. *Angiogenesis* **24**, 719–753 (2021).
4. Rosen, S. D., Singer, M. S., Yednock, T. A. & Stoolman, L. M. Involvement of sialic acid on endothelial cells in organ-specific lymphocyte recirculation. *Science* **228**, 1005–1007 (1985).

5. True, D. D., Singer, M. S., Lasky, L. A. & Rosen, S. D. Requirement for sialic acid on the endothelial ligand of a lymphocyte homing receptor. *J. Cell Biol.* **111**, 2757–2764 (1990).
6. Yang, W. H., Nussbaum, C., Grewal, P. K., Marth, J. D. & Sperandio, M. Coordinated roles of ST3Gal-VI and ST3Gal-IV sialyltransferases in the synthesis of selectin ligands. *Blood* **120**, 1015–1026 (2012).
7. Homeister, J. W. *et al.* The $\alpha(1,3)$ fucosyltransferases FucT-IV and FucT-VII exert collaborative control over selectin-dependent leukocyte recruitment and lymphocyte homing. *Immunity* **15**, 115–126 (2001).
8. Kawashima, H. *et al.* *N*-acetylglucosamine-6-*O*-sulfotransferases 1 and 2 cooperatively control lymphocyte homing through L-selectin ligand biosynthesis in high endothelial venules. *Nat. Immunol.* **6**, 1096–1104 (2005).
9. Uchimura, K. *et al.* A major class of L-selectin ligands is eliminated in mice deficient in two sulfotransferases expressed in high endothelial venules. *Nat. Immunol.* **6**, 1105–1113 (2005).
10. Chou, H. H. *et al.* A mutation in human CMP-sialic acid hydroxylase occurred after the Homo-Pan divergence. *Proc. Natl. Acad. Sci. USA.* **95**, 11751–11756 (1998).
11. Kawano, T. *et al.* Molecular cloning of cytidine monophospho-*N*-acetylneuraminic acid hydroxylase: Regulation of species- and tissue-specific expression of *N*-glycolylneuraminic acid. *J. Biol. Chem.* **270**, 16458–16463 (1995).
12. Streeter, P. R., Rouse, B. T. & Butcher, E. C. Immunohistologic and functional characterization of a vascular addressin involved in lymphocyte homing into peripheral lymph nodes. *J. Cell Biol.* **107**, 1853–1862 (1988).
13. Yeh, J. C. *et al.* Novel sulfated lymphocyte homing receptors and their control by a Core1 extension $\beta(1,3)$ -*N*-acetylglucosaminyltransferase. *Cell* **105**, 957–969 (2001).
14. Hirakawa, J. *et al.* Novel anti-carbohydrate antibodies reveal the cooperative function of sulfated *N*- and *O*-glycans in lymphocyte homing. *J. Biol. Chem.* **285**, 40864–40878 (2010).
15. Arata-Kawai, H. *et al.* Functional contributions of *N*- and *O*-glycans to L-selectin ligands in murine and human lymphoid organs. *Am. J. Pathol.* **178**, 423–433 (2011).
16. Matsumura, R. *et al.* Novel antibodies reactive with sialyl lewis X in both humans and mice define its critical role in leukocyte trafficking and contact hypersensitivity responses. *J. Biol. Chem.* **290**, 15313–15326 (2015).
17. Mitsuoka, C. *et al.* Identification of a major carbohydrate capping group of the L-selectin ligand on high endothelial venules in human lymph nodes as 6-sulfo sialyl Lewis X. *J. Biol. Chem.* **273**, 11225–11233 (1998).
18. Kawashima, H. Generation of anti-sulfated glycan antibodies using sulfotransferase-deficient mice. *Methods Mol. Biol.* **1022**, 51–60 (2013).
19. Tangemann, K., Bistrup, A., Hemmerich, S. & Rosen, S. D. Sulfation of a high endothelial venule-expressed ligand for L-selectin: Effects on tethering and rolling of lymphocytes. *J. Exp. Med.* **190**, 935–942 (1999).
20. Tobisawa, Y., Imai, Y., Fukuda, M. & Kawashima, H. Sulfation of colonic mucins by *N*-acetylglucosamine 6-*O*-sulfotransferase-2 and its protective function in experimental colitis in mice. *J. Biol. Chem.* **285**, 6750–6760 (2010).
21. Gallatin, W. M., Weissman, I. L. & Butcher, E. C. A cell-surface molecule involved in organ-specific homing of lymphocytes. *Nature* **304**, 30–34 (1983).
22. Berg, E. L., Robinson, M. K., Warnock, R. A. & Butcher, E. C. The human peripheral lymph node vascular addressin is a ligand for LECAM-1, the peripheral lymph node homing receptor. *J. Cell Biol.* **114**, 343–349 (1991).
23. Hemmerich, S., Butcher, E. C. & Rosen, S. D. Sulfation-dependent recognition of high endothelial venules (HEV)-ligands by L-selectin and MECA 79, and adhesion-blocking monoclonal antibody. *J. Exp. Med.* **180**, 2219–2226 (1994).
24. Sassetti, C., Tangemann, K., Singer, M. S., Kershaw, D. B. & Rosen, S. D. Identification of podocalyxin-like protein as a high endothelial venule ligand for L-selectin: parallels to CD34. *J. Exp. Med.* **187**, 1965–1975 (1998).
25. Baumhüter, S. *et al.* Binding of L-selectin to the vascular sialomucin CD34. *Science* **262**, 436–438 (1993).
26. Lasky, L. A. *et al.* An endothelial ligand for L-selectin is a novel mucin-like molecule. *Cell* **69**, 927–938 (1992).
27. Hellings, P., Jorissen, M. & Ceuppens, J. L. The Waldeyer's ring. *Acta Otorhinolaryngol. Belg.* **54**, 237–241 (2000).
28. Abbas, A. K., Murphy, K. M. & Sher, A. Functional diversity of helper T lymphocytes. *Nature* **383**, 787–793 (1996).
29. Walker, J. A. & McKenzie, A. N. J. T_H2 cell development and function. *Nat. Rev. Immunol.* **18**, 121–133 (2018).
30. Boonpiyathad, T., Satitsuksanoa, P., Akdis, M. & Akdis, C. A. IL-10 producing T and B cells in allergy. *Semin. Immunol.* **44**, 101326 (2019).
31. Lan, F., Zhang, N., Bachert, C. & Zhang, L. Stability of regulatory T cells in T helper 2-biased allergic airway diseases. *Allergy* **75**, 1918–1926 (2020).
32. Nicholson, M. W., Barclay, A. N., Singer, M. S., Rosen, S. D. & van der Merwe, P. A. Affinity and kinetic analysis of L-selectin (CD62L) binding to glycosylation-dependent cell-adhesion molecule-1. *J. Biol. Chem.* **273**, 763–770 (1998).
33. Arbonés, M. L. *et al.* Lymphocyte homing and leukocyte rolling and migration are impaired in L-selectin-deficient mice. *Immunity* **1**, 247–260 (1994).
34. Berlin, C. *et al.* $\alpha\beta 7$ integrin mediates lymphocyte binding to the mucosal vascular addressin MAdCAM-1. *Cell* **74**, 185–195 (1993).
35. Wagner, N. *et al.* L-selectin and $\beta 7$ integrin synergistically mediate lymphocyte migration to mesenteric lymph nodes. *Eur. J. Immunol.* **28**, 3832–3839 (1998).
36. Ohmichi, Y., Hirakawa, J., Imai, Y., Fukuda, M. & Kawashima, H. Essential role of peripheral node addressin in lymphocyte homing to nasal-associated lymphoid tissues and allergic immune responses. *J. Exp. Med.* **208**, 1015–1025 (2011).
37. Kiyono, H. & Fukuyama, S. NALT-versus Peyer's-patch-mediated mucosal immunity. *Nat. Rev. Immunol.* **4**, 699–710 (2004).
38. Paul, W. E. History of interleukin-4. *Cytokine* **75**, 3–7 (2015).
39. Ruddle, N. H. Lymphatic vessels and tertiary lymphoid organs. *J. Clin. Invest.* **124**, 953–959 (2014).
40. Jones, G. W., Hill, D. G. & Jones, S. A. Understanding immune cells in tertiary lymphoid organ development: It is all starting to come together. *Front. Immunol.* **7**, 401 (2016).
41. Pipi, E. *et al.* Tertiary lymphoid structures: Autoimmunity goes local. *Front. Immunol.* **9**, 1952 (2018).
42. Luo, S. *et al.* Chronic inflammation: A common promoter in tertiary lymphoid organ neogenesis. *Front. Immunol.* **10**, 2938 (2019).
43. Manzo, A., Bombardieri, M., Humby, F. & Pitzalis, C. Secondary and ectopic lymphoid tissue responses in rheumatoid arthritis: From inflammation to autoimmunity and tissue damage/remodeling. *Immunol. Rev.* **233**, 267–285 (2010).
44. Barone, F. *et al.* Association of CXCL13 and CCL21 expression with the progressive organization of lymphoid-like structures in Sjögren's syndrome. *Arthritis Rheum.* **52**, 1773–1784 (2005).
45. Suzawa, K. *et al.* Preferential induction of peripheral lymph node addressin on high endothelial venule-like vessels in the active phase of ulcerative colitis. *Am. J. Gastroenterol.* **102**, 1499–1509 (2007).
46. Kilkenny, C., Browne, W. J., Cuthill, I. C., Emerson, M. & Altman, D. G. Improving bioscience research reporting: The ARRIVE guidelines for reporting animal research. *PLoS Biol.* **8**, e1000412 (2010).

Acknowledgements

We would like to thank Dr. Yasuyuki Imai, Dr. Ryuji Matsumura, Dr. Koichiro Tsuboi, Dr. Hirohito Abo, Ms. Qianqian Liu, and Ms. Qiaofei Zhang for their helpful discussions and technical assistance with this study. We would also like to thank Core H of the Consortium for Functional Glycomics for performing the glycan array analysis.

Author contributions

H.K. conceived the idea for this project and designed the experiments. Wei L., W.X., Wenxin L., and H.K. performed the experiments and analyzed the data. J.H. provided critical support for the experiments. The manuscript was written by Wei L., W.X., and H.K.

Competing interests

This study was supported in part by the Japan Agency for Medical Research and Development (AMED; Grant Numbers 20ae0101034h0005, 22ae0121017h0002, and 22ym0126065h0001 to H.K.), JSPS KAKENHI (Grant Number 20H03379 to H.K.), and Institute for Advanced Academic Research of Chiba University (to H.K.). H.K. is an inventor on a PCT patent application (PCT/JP2021/036893) regarding the development and application of SF1 antibody filed by Chiba University. The other authors declare that they have no competing interests with the contents of this article.

Additional information

Supplementary Information The online version contains supplementary material available at <https://doi.org/10.1038/s41598-023-43017-w>.

Correspondence and requests for materials should be addressed to H.K.

Reprints and permissions information is available at www.nature.com/reprints.

Publisher's note Springer Nature remains neutral with regard to jurisdictional claims in published maps and institutional affiliations.



Open Access This article is licensed under a Creative Commons Attribution 4.0 International License, which permits use, sharing, adaptation, distribution and reproduction in any medium or format, as long as you give appropriate credit to the original author(s) and the source, provide a link to the Creative Commons licence, and indicate if changes were made. The images or other third party material in this article are included in the article's Creative Commons licence, unless indicated otherwise in a credit line to the material. If material is not included in the article's Creative Commons licence and your intended use is not permitted by statutory regulation or exceeds the permitted use, you will need to obtain permission directly from the copyright holder. To view a copy of this licence, visit <http://creativecommons.org/licenses/by/4.0/>.

© The Author(s) 2023